comparison with the order of magnitude of the other terms in Eqs. (10–12) it then becomes apparent that these pressure derivative terms can be neglected in the instantaneous equations of motion for a thin boundary layer except perhaps for low Mach number conditions near the wall. Since $R_\delta > 10^3$ for typical turbulent boundary layers,[15] the viscous terms are also negligible, but would have to be retained to insure the correct boundary conditions on velocities and enthalpy. Of course, very close to the wall, u, v, and $w \to 0$ as $y \to 0$, while the pressure derivative terms remain finite. Thus, to compute the details of the instantaneous motion very close to the wall, the pressure derivate terms in Eqs. (10–12) would also be required. These derivatives of the fluctuating pressure would balance fluctuations in the viscous terms. Subject to these restrictions on the pressure fluctuations, Eqs. (13) are then solutions to the instantaneous equations of motion when u_e, w_e, H_e, and H_w are constants and when $Pr = 1.0$.

Conclusions

The only restrictions on the application of Crocco's solution ($\bar{\theta} = \bar{F}$) and the independence principle ($\bar{g} = \bar{F}$) to boundary-layer flows, besides those just considered for the pressure fluctuations, are that u_e, w_e, and H_w must all be constant, $\bar{p} = \bar{p}(y)$ only, and $Pr = 1.0$. Since Eqs. (8) are now also applicable, an eddy diffusivity formulation for these conditions would require that the "total" turbulent Prandtl number[6] be unity and also that the eddy viscosity for the shear in the x and z directions be identical. It is also of interest to note that the "invariant turbulence" concept[10] used to model the eddy viscosity for swept cylinder flows[12] reduces to the correct form, consistent with the present analysis, for a swept flat plate. Morkovin's "Strong Reynolds Analogy" concept which was obtained[14] by extending the solutions $\bar{\theta} = \bar{F}$ and $\theta' = F'$ to the surface, can now be expected to apply better for $M > 4$ than at lower Mach numbers where the pressure fluctuation terms may become significant for $y \to 0$. Recent experimental data[18,19] tend to confirm this expectation for the ratio of surface heat transfer to skin friction. One can speculate further that this and other consequences of the Strong Reynolds Analogy may apply better in free flight than in noisy wind tunnels where facility generated noise may become nearly as large as p_w' measured under turbulent boundary layers.[20–22] However, Morkovin's application of this concept to adiabatic flows, wherein $H' = O$ (Ref. 14), is excluded in the present analysis by the requirement that $H_w \neq H_e$.

By use of the same analysis as given previously, it can be easily shown, subject to the restrictions just enumerated, that the Crocco solution applies to two-dimensional or quasi-two-dimensional flows including axisymmetric flows. The restriction of $Pr = 1.0$ is not required for the independence principle to apply to incompressible flow on a flat plate since, for constant density, the energy Eq. (3) is uncoupled from the momentum Eqs. (1) and (2). However, for incompressible flow, the pressure fluctuation terms Eq. (14) may not be negligible close to the wall. The experimental results of Ashkenas and Riddell[9] seem to favor this possibility that the independence principle does not apply accurately to the incompressible turbulent boundary layer on a yawed flat plate, especially in the region close to the wall.

References

[1] Van Driest, E. R., "Turbulent Boundary Layer in Compressible Fluids," *Journal of Aeronautical Sciences*, Vol. 18, No. 3, March 1951, pp. 145–160, 216.

[2] Crocco, L., "Sulla Transmissione del Calore da una Lamina Piana a un Fluido Scorrente adalta Velocita," *Aerotecnia*, Vol. 12, 1932, pp. 181–197.

[3] Schaubauer, G. B. and Tchen, C. M., "Turbulent Flows," *Turbulent Flows and Heat Transfer*, edited by C. C. Lin, Vol. V, *High Speed Aerodynamics and Jet Propulsion*, Princeton Univ. Press, Princeton, N.J., 1959, p. 91.

[4] Bushnell, D. M., Johnson, C. B., Harvey, W. D., and Feller, W. V., "Comparison of Prediction Methods and Studies of Relaxation in Hypersonic Turbulent Nozzle-Wall Boundary Layers," TN D-5620, 1969, NASA.

[5] Hopkins, E. J. and Kenner, E. R., "Pressure-Gradient Effects on Hypersonic Turbulent Skin Friction and Boundary-Layer Profiles," *AIAA Journal*, Vol. 10, No. 9, Sept. 1972, pp. 1141–1142.

[6] Bushnell, D. M. and Beckwith, I. E., "Calculation of Non-equilibrium Hypersonic Turbulent Boundary Layers and Comparisons with Experimental Data," *AIAA Journal*, Vol. 8, No. 8, Aug. 1970, pp. 1462–1469.

[7] Feller, W. V., "Effects of Upstream Wall Temperatures on Hypersonic Tunnel Wall Boundary-Layer Profile Measurements," *AIAA Journal*, Vol. 11, No. 4, April 1973, pp. 556–558.

[8] Jones, R. T., "Effects of Sweep Back on Boundary Layer and Separation," Rept. 884, 1947, NACA (supersedes NACA TN 1402).

[9] Ashkenas, H. and Riddell, F. R., "Investigation of the Turbulent Boundary Layer on a Yawed Flat Plate," TN 3383, 1955, NACA.

[10] Hunt, J. L., Bushnell, D. M., and Beckwith, I. E., "The Compressible Turbulent Boundary Layer on a Blunt Swept Slab With and Without Leading Edge Blowing," TN D-6203, March 1971, NASA.

[11] Schlichting, H., *Boundary Layer Theory*, 6th ed., McGraw-Hill, New York, 1968, p. 240.

[12] Hixon, B. A., Beckwith, I. E., and Bushnell, D. M., "Computer Program for Compressible Laminar or Turbulent Nonsimilar Boundary Layers," TM X-2140, April 1971, NASA.

[13] *Modern Developments in Fluid Mechanics, High Speed Flow*, edited by L. Howarth, Oxford Press, New York, 1953, pp. 454–455.

[14] Morkovin, M. V., "Effects of Compressibility on Turbulent Flows," *The Mechanics of Turbulence*, Gordon and Breach Scientific Publishers, Inc., 1964, pp. 367–380.

[15] Harvey, W. D., Bushnell, D. M., and Beckwith, I. E., "Fluctuating Properties of Turbulent Boundary Layers for Mach Numbers Up to 9," TN D-5496, 1969, NASA.

[16] Lawson, M. V., "Pressure Fluctuations in Turbulent Boundary Layers," TN D-3156, Dec. 1965, NASA.

[17] Fischer, M. C., Maddalon, D. V., Weinstein, L. M., and Wagner, R. D., "Bounday-Layer Pitot and Hot-Wire Surveys at $M_\infty \approx 20$," *AIAA Journal*, Vol. 9, No. 5, May 1971, pp. 826–834.

[18] Holden, M. S., "An Experimental Investigation of Turbulent Boundary Layers at High Mach Numbers and Reynolds Numbers," NASA CR-112147, Nov. 1972, Fig. 15, Cornell Aeronautical Lab., Buffalo, N.Y.

[19] Keener, E. R. and Polek, T. E., "Measurements of Reynolds Analogy for a Hypersonic Turbulent Boundary Layer on a Non-adiabatic Flat Plate," *AIAA Journal*, Vol. 10, No. 6, June 1972, pp. 845–846.

[20] Stainback, P. C., Fischer, M. C., and Wagner, R. D., "Effects of Wind-Tunnel Disturbances on Hypersonic Boundary-Layer Transition," AIAA Paper 72-181, San Diego, Calif., 1972, pt. I, Fig. 7.

[21] McCanless, G. F., Jr., "Aeronautical Noise Suppression at Transonic Mach Numbers," NASA CR-123810, May 1972, Fig. 8, Chrysler Corp., Huntsville Div., Huntsville, Ala.

[22] Dods, J. B., Jr. and Hanly, R. D., "Evaluation of Transonic and Supersonic Wind-Tunnel Background Noise and Effects of Surface Pressure Fluctuation Measurements," AIAA Paper 72-1004, Palo Alto, Calif., 1972, Fig. 11.

Finite Twisting and Bending of Thin Orthotropic Strip of Lenticular Section

C. H. S. Chen*

The B. F. Goodrich Co., Arkon, Ohio

THE large-deflection solution for a thin strip of lenticular parabolic section made of isotropic material when subjected to combined moment M and torque T was obtained by

Received July 30, 1973; revision received August 30, 1973. Presented at 4th Canadian Congress of Applied Mechanics, Montreal, Canada, May 1973, as part of the paper entitled "Finite Twisting and Bending of Thin Orthotropic Elastic Strip."

Index categories: Structural Stability Analysis; Structural Composite Materials (Including Coatings).

* Senior Engineering Scientist. Member AIAA.

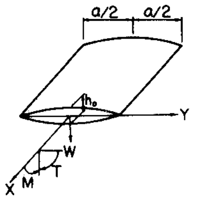

Fig. 1 Strip of lenticular section.

Mansfield.[1,2] His analysis includes the buckled as well as unbuckled regions and the tendency of the surface to deform into a developable surface after buckling is discussed. In the present work the solution of Mansfield is extended to the strip of orthotropic material whose axes of elastic symmetry coincide with the geometric axes of symmetry of the strip.

Following the work of Mansfield we also assume the deflection and force functions to be

$$w(x, y) = -\tfrac{1}{2}ky^2 - \theta xy + W(y) \tag{1}$$

$$\Phi(x, y) = \Phi(y) \tag{2}$$

For a strip of lenticular parabolic section, we have (see Fig. 1)

$$h = h_o[1-(2y/a)^2]$$

$$D_i = D_{io}[1-(2y/a)^2]^3$$

where $i = x, y, 1$ or xy and $D_{io} = D_i(h_o)$ with

$$D_x = E_x h_o^3/12(1-\nu_{xy}\nu_{yx}), \qquad D_y = E_y h_o^3/12(1-\nu_{xy}\nu_{yx})$$

$$D_{xy} = G_{xy}h_o^3/12, \qquad D_1 = D_x\nu_{yx} = D_y\nu_{xy}$$

Going through the same procedures as Mansfield did, we will obtain

$$\hat{U} = \tfrac{1}{2}\hat{k}^2 + \frac{2G_{xy}}{E_x}\hat{\theta}^2 + \frac{(\hat{\theta}^2+\nu_{xy}\hat{k}^2)^2}{2[1+(1-\nu_{xy}\nu_{yx})(E_x/E_y)\hat{k}^2]} \tag{3}$$

$$\hat{k}' = -\left[\frac{\nu_{xy}-(1-\nu_{xy}\nu_{yx})(E_x/E_y)\hat{\theta}^2}{1+(1-\nu_{xy}\nu_{yx})(E_x/E_y)\hat{k}^2}\right]\hat{k} \tag{4}$$

$$\hat{N} = -[\hat{\theta}^2+\nu_{xy}\hat{k}^2/1+(1-\nu_{xy}\nu_{yx})(E_x/E_y)\hat{k}^2] \tag{5}$$

$$\hat{M} = \frac{\partial\hat{U}}{\partial\hat{k}} = \frac{\hat{k}}{[1+(1-\nu_{xy}\nu_{yx})(E_x/E_y)\hat{k}^2]^2}\times \left\{\left[1+(1+\nu_{xy})\left(\frac{E_x}{E_y}\hat{k}^2+\hat{\theta}^2\right)\right]\left[1+(1-\nu_{xy})\left(\frac{E_x}{E_y}\hat{k}^2-\hat{\theta}^2\right)\right]+ (\nu_{yx}-\nu_{xy})\left(\frac{E_x}{E_y}\right)^2\hat{k}^4+\left[(1-\nu_{xy}\nu_{yx})\left(1-\frac{E_x}{E_y}\right)+\nu_{xy}-\nu_{yx}\right]\hat{\theta}^4\right\} \tag{6}$$

$$\hat{T} = \frac{E_x}{4G_{xy}}\frac{\partial\hat{U}}{\partial\hat{\theta}} = \frac{\hat{\theta}\left\{1+\left[(1-\nu_{xy}\nu_{yx})\frac{E_x}{E_y}+\frac{E_x}{G_{xy}}\frac{\nu_{xy}}{2}\right]\hat{k}^2+\frac{E_x}{2G_{xy}}\hat{\theta}^2\right\}}{1+(1-\nu_{xy}\nu_{yx})\frac{E_x}{E_y}\hat{k}^2} \tag{7}$$

where the nondimensional parameters (quantities with hats) are defined in the same manner as by Mansfield except that E_x and G_{xy} replace E and G, respectively.

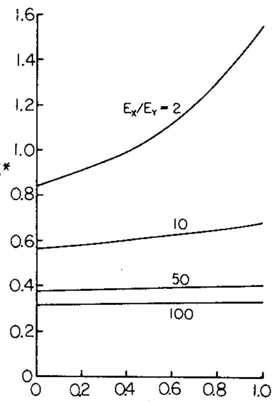

Fig. 2 Dimensionless critical twist as function of ν_{xy} for various values of E_x/E_y.

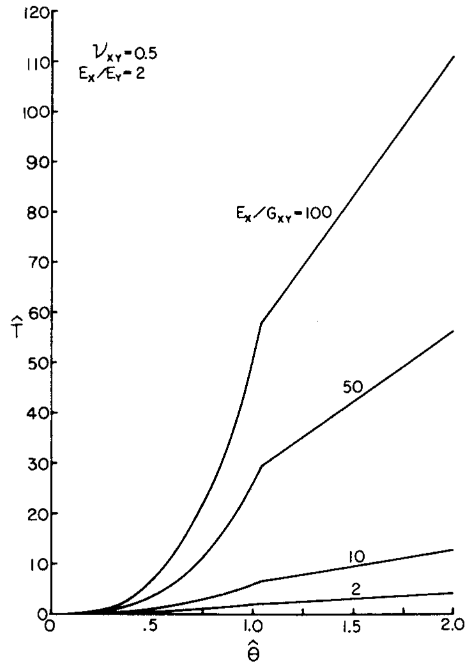

Fig. 3 Dimensionless torque as function of dimensionless twist for various values of E_x/G_{xy} when $\nu_{xy} = 0.5$, $E_x/E_y = 2$.

In the case of the strip under pure moment and suppose $(1-\nu_{xy}\nu_{yx}) \geq 0$, the condition that $\hat{T} = 0$ implies that $\hat{\theta} = 0$. Hence we have

$$\begin{aligned} \hat{M} &= \frac{\hat{k}}{1-\nu_{xy}\nu_{yx}}\left\{1-\frac{\nu_{xy}\nu_{yx}}{[1+(1-\nu_{xy}\nu_{yx})(E_x/E_y)\hat{k}^2]^2}\right\} \\ \hat{k}' &= [-\nu_{xy}\hat{k}/1+(1-\nu_{xy}\nu_{yx})(E_x/E_y)\hat{k}^2] \\ \hat{N} &= [-\nu_{xy}\hat{k}^2/1+(1-\nu_{xy}\nu_{yx})(E_x/E_y)\hat{k}^2] \end{aligned} \tag{8}$$

For large value of $\hat{k}$, relations (8) give us the conclusion identical to that of Mansfield. That is, the strip tends to a developable surface and midplane forces approach constant values.

For a strip under pure torque, the condition that $\hat{M} = 0$ implies that either

$$\hat{k} = 0 \tag{9}$$

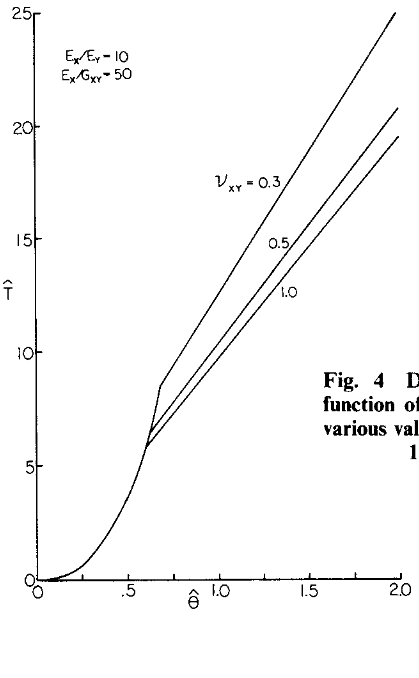

Fig. 4 Dimensionless torque as function of dimensionless twist for various values of ν_{xy} when $E_x/E_y = 10$, $E_x/G_{xy} = 50$.

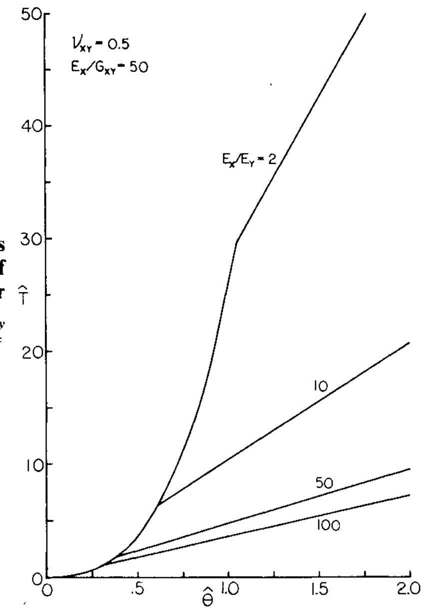

Fig. 5 Dimensionless torque as function of dimensionless twist for various values of E_x/E_y when $\nu_{xy} = 0.5$, $E_x/G_{xy} = 50$.

or

$$\hat{k}^4 + \frac{2}{(1-\nu_{xy}\nu_{yx})(E_x/E_y)}\hat{k}^2 - \frac{1}{(E_x/E_y)^4}\hat{\theta}^4 + \frac{2\nu_{xy}}{(1-\nu_{xy}\nu_{yx})(E_x/E_y)^2}\hat{\theta}^2 + \frac{1}{(1-\nu_{xy}\nu_{yx})(E_x/E_y)^2} = 0 \qquad (10)$$

In the first case

$$\hat{T} = \hat{\theta}[1+(E_x/2G_{xy})\hat{\theta}^2]$$
$$\hat{K}' = 0 \qquad (11)$$
$$\hat{N} = -\hat{\theta}^2$$

In the second case

$$\hat{k}^2 = \left|\frac{-1}{(1-\nu_{xy}\nu_{yx})(E_x/E_y)} + \frac{1}{(E_x/E_y)^{1/2}}\left(\hat{\theta}^2 - \frac{\nu_{yx}}{1-\nu_{xy}\nu_{yx}}\right)\right|$$
$$\hat{T} = \hat{\theta}\left\{1 + \frac{E_x}{2G_{xy}}\frac{1}{(1-\nu_{xy}\nu_{yx})(E_x/E_y)^{1/2}}\left[1+\frac{\nu_{xy}}{(E_x/E_y)^{1/2}}\right]\right\}$$
$$\hat{k}' = [1/(E_x/E_y)^{1/2}]\hat{k} \qquad (12)$$
$$\hat{N} = -\frac{1+[\nu_{xy}/(E_x/E_y)^{1/2}]}{(1-\nu_{xy}\nu_{yx})(E_x/E_y)^{1/2}}$$

It is found from a comparison of strain energies that Eqs. (11) are applicable for values of $|\hat{T}|$ up to critical value $\hat{T}^*$ where

$$\hat{T}^* = \hat{\theta}^*[1+(E_x/2G_{xy})(\hat{\theta}^*)^2] \qquad (13)$$

corresponding to the following critical angle of twist

$$\hat{\theta}^* = \left[\frac{1+[\nu_{xy}/(E_x/E_y)^{1/2}]}{(1-\nu_{xy}\nu_{yx})(E_x/E_y)^{1/2}}\right]^{1/2} \qquad (14)$$

Equations (12) are applicable for values of $|\hat{T}|$ greater than $\hat{T}^*$.

Figure 2 shows variations of $\hat{\theta}^*$ as function of ν_{xy} and E_x/E_y. As E_x/E_y increases, $\hat{\theta}^*$ becomes nearly independent of ν_{xy}. Figures 3–5 show curves of $\hat{T}$ vs $\hat{\theta}$ for different values of parameters E_x/G_{xy}, ν_{xy}, and E_x/E_y. The instability phenomenon at $\hat{\theta} = \hat{\theta}^*$ is due to the fact that as the strip is twisted the midplane force becomes more resisting to the torque and as a result the strip buckles and deforms into a surface which approximates to a developable surface.

References

[1] Mansfield, E. H., "The Large-Deflection Behavior of a Thin Strip of Lenticular Section," *Quarterly Journal of Mechanics and Applied Mathematics*, Vol. XII, No. 4, Nov. 1959, pp. 421–430.

[2] Mansfield, E. H., *The Bending and Stretching of Plates*, Pergamon Press, New York, 1964, Chap. VII.

[3] Lekhnitskii, S. G., *Anisotropic Plates*, Gordon and Breach, New York, 1968 (English Translation).

[4] Timoshenko, S. P. and Woinowsky-Krieger, S., *Theory of Plates and Shells*, 2nd ed., McGraw-Hill, New York, 1959.

Calculation of Mechanical Impedance by Finite Element Hybrid Model

S. T. Mau* and P. Tong†
MIT, Cambridge, Mass.

IN a recent paper,[1] the mechanical impedance of damped three-layer sandwich rings (Fig. 1) are calculated using series solution. The governing differential equations are reduced to simple algebraic equations by assuming trigonometric series for the displacements. For a problem of rather simple geometry given in Ref. 1, the analytical derivation is already rather lengthy. For problems of more complex geometry, it would be very difficult to obtain solutions. It should be recognized, however, that such problems can readily be solved by the finite element method regardless of their geometry complexity. Since the problem concerns only periodically forced vibration, the frequency-dependent viscous material properties can be expressed as complex constants which are functions of the forcing frequency. The finite element system equations can be written as

$$\mathbf{M}\ddot{\mathbf{u}} + \mathbf{K}\mathbf{u} = \mathbf{f}\,e^{i\omega t} \qquad (1)$$

where **M** and **K** are system mass and stiffness matrices, and **u** and **f** are displacement force vectors, respectively. By assuming

$$\mathbf{u} = \mathbf{u}_0\,e^{i\omega t} \qquad (2)$$

Eq. (1) becomes

$$(\mathbf{K} - \omega^2\mathbf{M})\mathbf{u}_0 = \mathbf{f} \qquad (3)$$

Thus the response vector $\mathbf{u}_0$ can be easily solved for any given ω. Since the material constants of the sandwich core are complex and a function of frequency, the stiffness matrix **K** is also complex and frequency dependent and the vector $\mathbf{u}_0$ is also complex. Once the complex $\mathbf{u}_0$ is obtained, the velocity $\dot{\mathbf{u}}$ can be calculated by

$$\dot{\mathbf{u}} = i\omega\mathbf{u}_0\,e^{i\omega t} \qquad (4)$$

and the mechanical impedance, which is the ratio of the amplitude of the force to the amplitude of the velocity at a point, can be calculated accordingly. The preceding solution procedure has been applied to sandwich beam problems using displacement elements.[2]

In this Note, the same procedure is applied, using a multilayer hybrid stress quadrilateral flat plate element,[3,4] to one of the sandwich ring problems solved in Ref. 1. The adaptation of complex material constants for the hybrid stress element is just as easy as that for a displacement element.

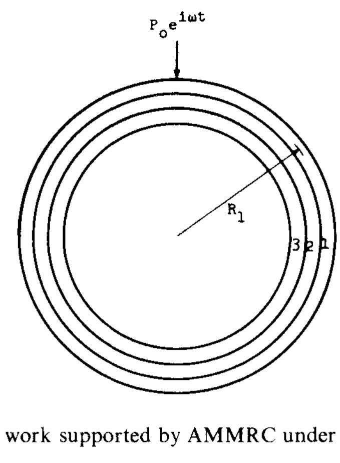

Fig. 1 Geometry and loading of the three layer sandwich ring.

Received August 3, 1973. This work supported by AMMRC under contract DAAG 46-73-C-0090.

Index categories: Structural Dynamic Analysis; Structural Composite Materials (Including Coatings).

* Senior Research Engineer, Aeroelastic and Structures Research Laboratory.

† Associate Professor.